Quench Dynamics for Trapped Dipolar Fermi Gases

Vladimir Veljić[1], Antun Balaž[1], and Axel Pelster[2]

[1]Scientific Computing Laboratory, Institute of Physics Belgrade, University of Belgrade, Serbia
[2]Physics Department and Research Center Optimas, Technical University of Kaiserslautern, Germany

Abstract

A recent time-of-flight expansion experiment for polarized fermionic erbium atoms managed to detect a Fermi surface deformation which is due to the dipolar interaction [1]. Here we perform a systematic study of quench dynamics of trapped dipolar Fermi gases at zero temperature, which are induced by a sudden change of the magnetic field, which enforces the polarization of the magnetic moments of the erbium atoms. As this modifies the equilibrium configuration, oscillations of the fermionic erbium cloud emerge around the new equilibrium, which are characteristic for the presence of the dipole-dipole interaction. In order to analyze the emergent dynamics we follow Ref. [2] and solve analytically the Boltzmann-Vlasov equation within the relaxation approximation in the vicinity of the new equilibrium configuration by using a suitable rescaling of the equilibrium distribution [3]. The resulting ordinary differential equations of motion for the scaling parameters are solved numerically for experimentally relevant parameters in the collisionless regime. A comparison with a corresponding linear stability analysis reveals that the resulting quench dynamics can be understood in terms of the low-lying collective modes due to the smallness of the dipolar interaction strength. All our theoretical and numerical calculations can be tested in current experiments with ultracold dipolar fermionic atoms.

Experiment

- ⋆ The sample in experiment [1] contains $N = 7 \cdot 10^4$ fermionic ^{167}Er atoms
- ⋆ Atoms are confined into harmonic trap with frequencies $(\omega_x, \omega_y, \omega_z) = 2\pi(579, 91, 611)$ Hz
- ⋆ The atomic cloud is imaged with an angle of $\alpha = 28^\circ$ with respect to the y-axis

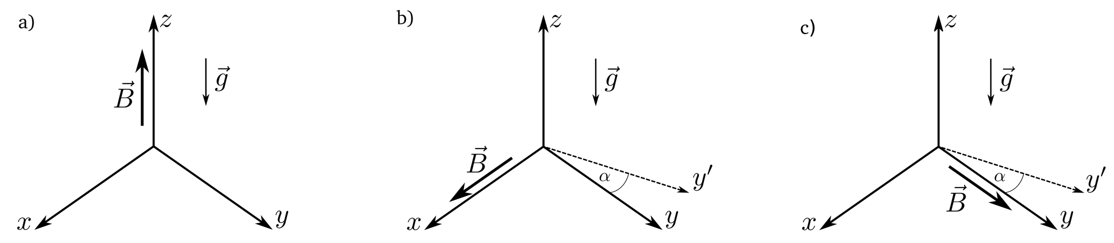

Fig. 1. (a) Experimental setup in Ref. [1]; (b) case 1: $z \to x$ quench; (c) case 2: $z \to y$ quench

Equations

- ⋆ The total number of fermions is:

$$N = \frac{1}{48} R_x R_y R_z K_x K_y K_z \,,$$

where R_i and K_i represent variational parameters for the Thomas-Fermi radii and momenta, respectively

- ⋆ Static equations for the parameters K_i and R_i before the quench:

$$K_x = K_y \,,$$

$$\frac{\hbar^2 K_z^2}{2m} - \frac{\hbar^2 K_x^2}{2m} = -\frac{3}{2}\frac{48 N c_0}{\prod_j R_j}\left[-1 + \frac{\left(2K_x^2 + K_z^2\right) f_{\mathrm{s}}\left(\frac{K_z}{K_x}\right)}{2\left(K_x^2 - K_z^2\right)}\right] ,$$

$$\omega_x^2 R_x^2 - \frac{1}{3}\sum_j \frac{\hbar^2 K_j^2}{m^2} + \frac{48 N c_0}{m \overline{R}^3}\left[f\left(\frac{R_x}{R_z}, \frac{R_y}{R_z}\right) - f_{\mathrm{s}}\left(\frac{K_z}{K_x}\right) - \frac{R_x}{R_z} f_1\left(\frac{R_x}{R_z}, \frac{R_y}{R_z}\right)\right] = 0 \,,$$

$$\omega_y^2 R_y^2 - \frac{1}{3}\sum_j \frac{\hbar^2 K_j^2}{m^2} + \frac{48 N c_0}{m \overline{R}^3}\left[f\left(\frac{R_x}{R_z}, \frac{R_y}{R_z}\right) - f_{\mathrm{s}}\left(\frac{K_z}{K_x}\right) - \frac{R_y}{R_z} f_2\left(\frac{R_x}{R_z}, \frac{R_y}{R_z}\right)\right] = 0 \,,$$

$$\omega_z^2 R_z^2 - \frac{1}{3}\sum_j \frac{\hbar^2 K_j^2}{m^2} + \frac{48 N c_0}{m \overline{R}^3}\left[f\left(\frac{R_x}{R_z}, \frac{R_y}{R_z}\right) - f_{\mathrm{s}}\left(\frac{K_z}{K_x}\right) + \frac{R_x}{R_z} f_1\left(\frac{R_x}{R_z}, \frac{R_y}{R_z}\right) + \frac{R_y}{R_z} f_2\left(\frac{R_x}{R_z}, \frac{R_y}{R_z}\right)\right] = 0 \,,$$

where f denotes the anisotropy function [2]

- ⋆ Static equations after $z \to x$ and $z \to y$ quench can be obtained by permuting indices in static equations before the quench according to the rules: $\{x \to y,\, y \to z,\, z \to x\}$ and $\{x \to z,\, y \to x,\, z \to y\}$
- ⋆ Boltzmann-Vlasov equation in the vicinity of the new equilibrium configuration (after the quench) is solved by using a suitable rescaling ansatz of the equilibrium distribution [3]
- ⋆ Equations of motion for scaling parameter b_i after $z \to x$ quench in the collisionless regime:

$$\ddot{b}_i + \omega_i^2 b_i - \frac{\hbar^2 K_i^2 \theta_i}{m^2 b_i R_i^2} + \frac{48 N c_0}{m b_i R_i^2 \prod_j b_j R_j}\left[f\left(\frac{b_y R_y}{b_x R_x}, \frac{b_z R_z}{b_x R_x}\right) - b_i R_i \frac{\partial}{\partial b_i R_i} f\left(\frac{b_y R_y}{b_x R_x}, \frac{b_z R_z}{b_x R_x}\right)\right]$$

$$-\frac{48 N c_0}{m b_i R_i^2 \prod_j b_j R_j}\left[f\left(\frac{b_y K_x}{b_x K_y}, \frac{b_z K_x}{b_x K_z}\right) + \frac{K_i}{b_i}\frac{\partial}{\partial K_i b_i} f\left(\frac{b_y K_x}{b_x K_y}, \frac{b_z K_x}{b_x K_z}\right)\right] = 0 \,,$$

- ⋆ Equations for scaling parameter b_i after $z \to y$ quench can be obtained by permuting indices in above equations according to the following rule: $\{x \to y,\, y \to z,\, z \to x\}$
- ⋆ Differential equations for $b_i(t)$ are solved numericaly with inital conditions $b_i(0) = R_{bi}/R_{ai}$, where indices b and a denote the values of static parameters before and after the quench

Quench Dynamics in Momentum Space

- ⋆ Dynamics in the momentum space can be described in terms of aspect ratios $A_{Ki}(t) = \sqrt{\langle k_i^2 \rangle / \langle k_z^2 \rangle}$, where expectation values are given by:

$$\langle k_i^2 \rangle = \frac{1}{8}\left(\frac{K_{ai}^2}{b_i^2(t)} + \frac{m^2 R_{ai}^2 \dot{b}_i^2(t)}{\hbar^2}\right)$$

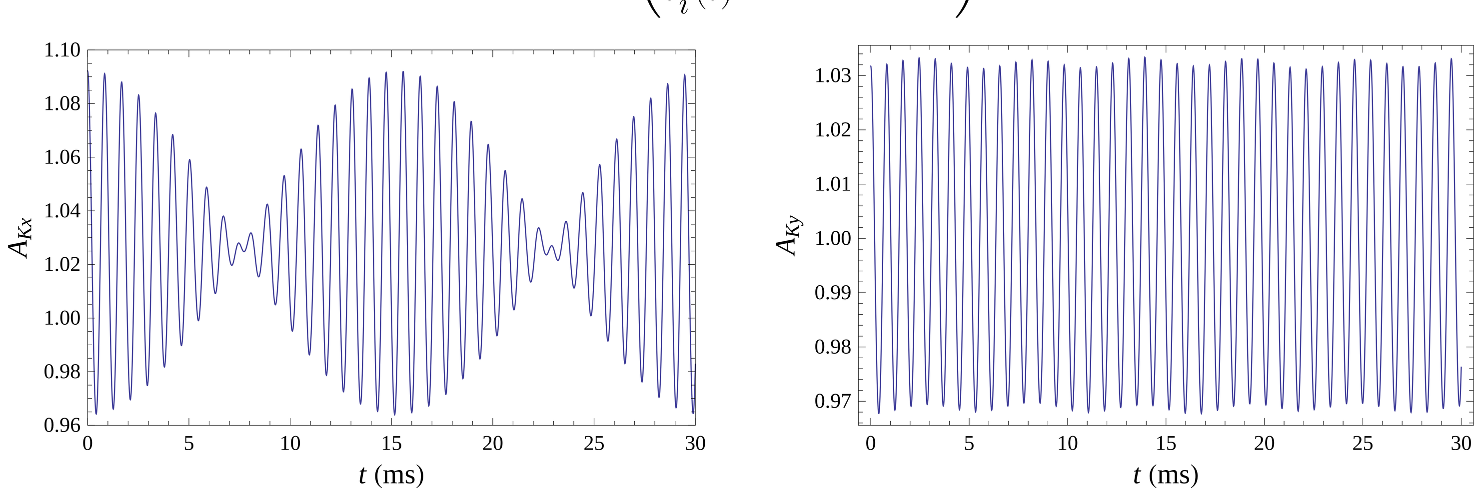

Fig. 2. Aspect ratios in the momentum space after $z \to x$ quench.

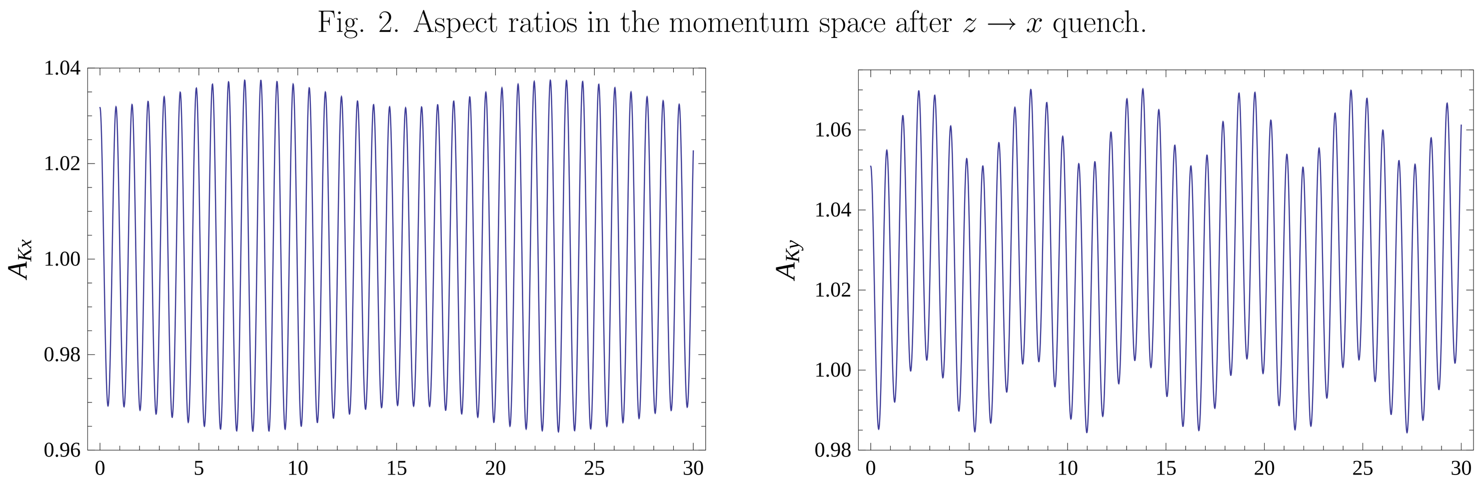

Fig. 3. Aspect ratios in the momentum space after $z \to y$ quench.

Quench Dynamics in Real Space

- ⋆ Dynamics in the real space can be described in terms of scaling parameters b_i and aspect ratio $A_R(t)$:

$$A_R(t) = \sqrt{\frac{\langle r_z^2 \rangle}{\langle r_x^2 \rangle \cos^2\alpha + \langle r_y^2 \rangle \sin^2\alpha}} = \frac{R_{az} b_z(t)}{\sqrt{R_{ax}^2 b_x^2(t) \cos^2\alpha + R_{ay}^2 b_y^2(t) \sin^2\alpha}}$$

Case 1: $z \to x$ quench

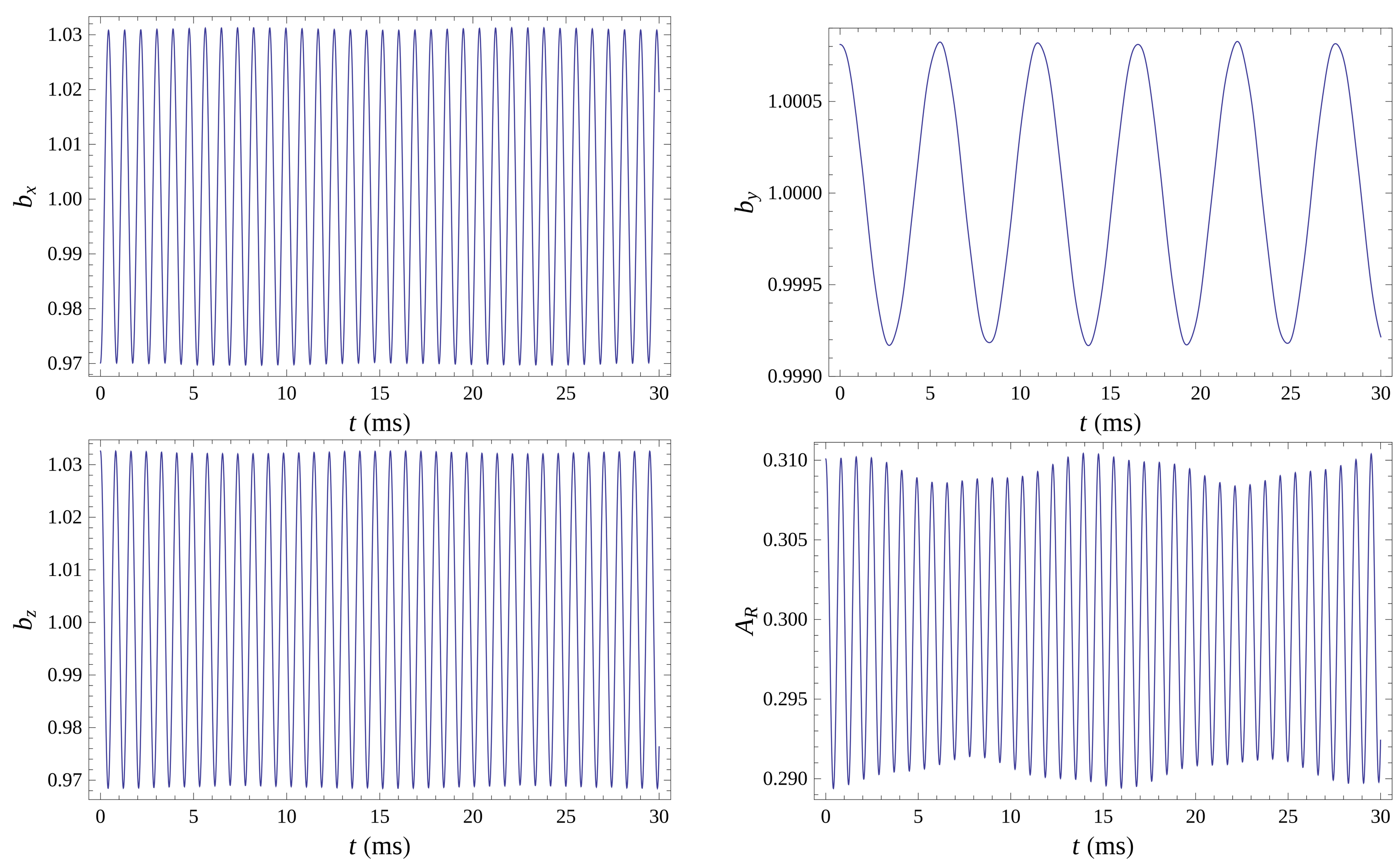

Fig. 4. Time evolution of b_i and A_R after $z \to x$ quench.

- ⋆ Using Fourier transformation we get dominant oscillation frequencies for $b_i(t)$ for $z \to x$ quench:

$$\Omega_x = 1154 \cdot 2\pi \text{ Hz} \,,$$
$$\Omega_y = 181 \cdot 2\pi \text{ Hz} \,,$$
$$\Omega_z = 1220 \cdot 2\pi \text{ Hz} \,.$$

Case 2: $z \to y$ quench

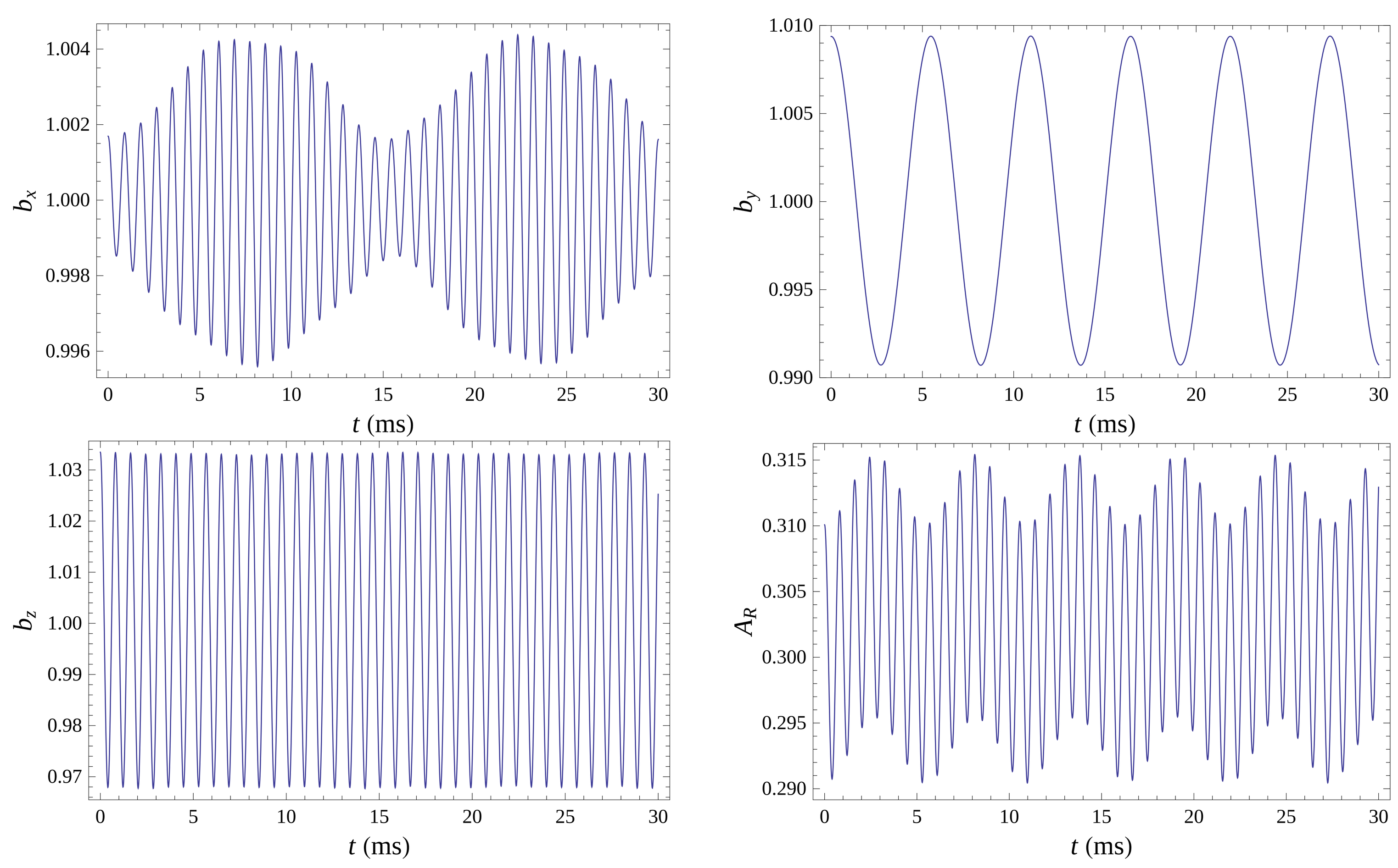

Fig. 5. Time evolution of b_i and A_R after $z \to y$ quench.

- ⋆ Using Fourier transformation we get dominant oscillation frequencies for $b_i(t)$ for $z \to y$ quench:

$$\Omega_x = 1165 \cdot 2\pi \text{ Hz} \,,$$
$$\Omega_y = 185 \cdot 2\pi \text{ Hz} \,,$$
$$\Omega_z = 1230 \cdot 2\pi \text{ Hz} \,.$$

Conclusions and Outlook

- ⋆ Quench dynamics is a consequence of dipole-dipole interaction
- ⋆ Dominant frequencies of the oscillations are nearly twice the trap frequencies $\Omega_i \approx 2\omega_i$
- ⋆ Study of time-of-flight images obtained for various holding times after the quench
- ⋆ Eigenvectors and eigenfrequencies for collective oscillation modes: from collisionless to hydrodynamic regime
- ⋆ Development of the formalism for arbitrary magnetic field and imaging direction

References

[1] K. Aikawa, S. Baier, A. Frisch, M. Mark, C. Ravensbergen, and F. Ferlaino, Science **345**, 1484 (2014).
[2] F. Wächtler, A. R. P. Lima, and A. Pelster, `arXiv:1311.5100` (2013).
[3] P. Pedri, D. Guery-Odelin, and S. Stringari, Phys. Rev. A **68**, 043608 (2003).

Acknowledgments: We gratefully acknowledge support by DAAD - German Academic and Exchange Service under project IBEC, Ministry of Education, Science, and Technological Development of the Republic of Serbia under projects ON171017 and IBEC, and German Research Foundation (DFG) via the Collaborative Research Center SFB/TR49.